論文 / 著書情報
Article / Book Information

論題	
Title	Analysis of single- and double-barrier tunneling diode structures using ultrathin CaF₂/CdF₂/Si multilayered heterostructures grown on Si
著者	須田 慶太, 桑田 友哉, 渡辺 正裕
Authors	Keita Suda, Yuya Kuwata, Masahiro Watanabe
出典	, Vol. 54, No. 4S, 04DJ05-1
Citation	Jpn. J. Appl. Phys., Vol. 54, No. 4S, 04DJ05-1
発行日 / Pub. date	2015, 3
DOI	http://dx.doi.org/10.7567/JJAP.54.04DJ05
URL	http://iopscience.iop.org/1347-4065/
権利情報 / Copyright	本著作物の著作権は（公社）応用物理学会に帰属します。 (c) 2015 The Japan Society of Applied Physics
Note	このファイルは著者（最終）版です。 This file is author (final) version.

Analysis of single- and double-barrier tunneling diode structures using ultrathin $CaF_2/CdF_2/Si$ multilayered heterostructures grown on Si

Keita Suda*, Yuya Kuwata, and Masahiro Watanabe

Department of Electronics and Applied Physics, Interdisciplinary Graduate School of Science and Engineering, Tokyo Institute of Technology, Yokohama 226-8502, Japan

**E-mail: suda.k.ae@m.titech.ac.jp*

The current-voltage (I-V) characteristics of single-barrier and double-barrier tunneling diode structures using $CaF_2/CdF_2/Si$ ultrathin multilayered heterostructures grown on Si substrates have been theoretically analyzed and their material parameters, such as the conduction band discontinuity (ΔE_C) at the heterointerface and effective mass (m*), have been evaluated by fitting simulation with the measured I-V characteristics. ΔE_C between the ultrathin (1-3 nm) CaF_2 and Si layers and m* for CaF_2 were found to be 1.5 - 2.3 eV and 0.3-1.0 m_0, respectively. A clear thickness dependence of these parameters was observed, and the deviations of m* and ΔE_C were approximately 30-50%, which probably originated from the thin layer thicknesses in atomic order. Using the estimated values derived from the single-barrier tunneling diodes, m* for CdF_2 was also estimated to be 0.36 m_0 by fitting simulation of double-barrier diodes. These results will contribute to

clarifying the design principle of tunneling devices with CaF_2 and enhancing quantitative studies on electron transport in atomically thin multilayered heterostructures.

1. Introduction

The dimensions of the elements making up integrated circuits are reduced to nanoscale. One essential building block for nanoscale solid-state devices is the electric potential sequences for controlling electron transport, which can be implemented using the energy band discontinuity at atomically abrupt heterointerfaces. A $CaF_2/CdF_2/Si$ heterostructure is an attractive candidate structure for applications in Si substrates, such as resonant tunneling diodes (RTDs) [1,2] and transistors [3], and resistance switching devices [4,5], because of the large conduction band discontinuity (ΔE_C~2.3 eV for Si/CaF_2) at the heterointerface [6] and the small lattice mismatch with silicon. To date, we have demonstrated high ON/OFF current ratios greater than 10^5 for CdF_2/CaF_2 RTDs at room temperature (RT) [1,7,8], which confirmed the advantage of large-ΔE_C heterostructure material systems. To establish a design paradigm for tunneling devices using heterostructure materials, the modeling of electron transport and key material parameters, such as the conduction band discontinuity and effective masses for atomically thin layers, is essential for the design and optimization of device performance. It has been reported that ΔE_C between Si and a few-monolayer-thick CaF_2 layer is significantly smaller than that for a bulk CaF_2 layer [9-11] investigated mainly by a scanning-tunneling-spectroscopy-based technique, and that ΔE_C should be sensitive to the tunneling current density. In this study, we have carried out a systematic fitting simulation of the I-V characteristics of single-barrier and double-barrier tunneling diode structures, focusing on the material parameters of ΔE_C and the effective mass (m*) of CaF_2, and determined the thickness dependences of these material parameters to establish a sophisticated design paradigm for electron transport through multilayered heterostructures including atomically thin CaF_2 layers.

2. Calculation method and sample preparation

The tunneling current was calculated using the transfer-matrix method and Esaki-Tsu formula [12, 13] assuming the effective mass approximation and self-consistent potential scheme [14-16]. The effect of the voltage drop due to the accumulation and depletion of carriers in the Si layer was considered in the calculation. Any scattering effect was neglected in this study in accordance with the ballistic transport approximation. Fitting simulations of I-V curves of Al/CaF_2/Si single-barrier and Si/CaF_2/CdF_2/CaF_2/Si double-barrier tunneling diode structures with ultrathin CaF_2 barrier layers (1 - 3 nm) were carried out. The CdF_2 quantum-well (QW) layer thickness was fixed at 2.5 nm. The parameters for the calculation are shown in Table I [17-19], and ΔE_C and m* for CaF_2 were the fitting parameters used.

In this study, for the single-barrier tunneling diodes, three samples with CaF_2 layers of different thicknesses (t_{CaF2} = 0.93, 1.6, and 2.2 nm) were fabricated on Si substrates. The thickness of the CaF_2 layer strongly affects the current density of the tunneling diode since the transfer coefficient of the tunneling barrier has an exponential dependence on the barrier thickness. For a double-barrier resonant tunneling diode, the measured I-V curve was obtained from Ref. 5. The fabrication processes of the single- and double-barrier diodes are based on common techniques briefly summarized as follows. A 40-nm-thick SiO_2 layer was formed on an n-type Si(111) substrate with a 0.1° off miscut angle and a resistivity of less than 4 mΩ·cm by pyrogenic oxidation. Subsequently, 2.2-μm-diameter holes were formed by photolithography followed by etching with buffered hydrogen fluoride solution (BHF), which produces a hydrogen-terminated Si surface. Subsequently, a protective oxide layer was formed on the Si surface at the bottom

of the holes by boiling in a mixed solution of hydrochloric acid and hydrogen peroxide (SC2). After loading into an ultrahigh-vacuum (UHV) chamber, a single layer of CaF_2 was grown on the bottom Si layer by a molecular-beam-epitaxy (MBE)-based technique. Details of the growth conditions of the layers are described in Refs. 4, 5, and 20–22. After unloading each sample from the UHV chamber, 200×200 μm^2 Au/Al electrode pads were formed by lift-off. I-V measurement was carried out using an Agilent B1500A device analyzer.

3. Results and discussion

Figure 1 shows the RT I-V characteristics of the single-barrier tunneling diodes with the CaF_2 barrier layers of (i) 0.93, (ii) 1.6, and (iii) 2.2 nm thicknesses, where the schematic conduction band profile is shown in the inset. Circles, squares, and triangles indicate measurement results. The solid and dashed lines indicate the calculated results fitted using the parameters (i) $m^* = 1.0\ m_0$ and ΔE_C=1.5 eV, (ii) $m^* = 0.7\ m_0$ and $\Delta E_C = 1.7$ eV, and (iii) $m^* = 0.5\ m_0$ and $\Delta E_C = 2.1$ eV, respectively, where m_0 indicates the free electron mass. The material parameters are shown in Table I. From the fitting simulation of lines (i)-(iii), the work function of Al was evaluated to be 4.37 eV, which minimizes the error of mean square. The measured I-V curves were well reproduced by the fitting simulation, as shown in the figure. Figure 2 shows the plots of the extracted values of ΔE_C and m^* as functions of the thickness of the CaF_2 barrier layer. It was found that ΔE_C decreases from 2.1 to 1.5 eV and m^* increases from 0.5 to 1.0 m_0 when the thickness of the CaF_2 layer ranges from 2.2 to 0.93 nm. In the case of ΔE_C between Si and CaF_2, a similar tendency was reported in Refs. 9–11, where the value was estimated by a scanning-tunneling-spectroscopy-based

technique. The obtained ΔE_C is 35% smaller than that for the reported bulk CaF_2-Si heterointerface (ΔE_C~2.3 eV) [17], which suggests that the deviation is due to the variation in the energy band structure of the atomically thin CaF_2. On the other hand, the deviation of m* as a function of layer thickness has not been reported, although Zhang et al. suggested that m* for 3.0-nm-thick CaF_2 is 0.3 m_0 in Ref. 23, and ΔE_C and m* for SiO_2 and Al_2O_3 have been widely studied from the viewpoint of the tunneling current through atomically thin insulators [24-29]. The tendency of the variation in m* shown in Fig. 2 seems to be almost linear as a function of ΔE_C, although the physical interpretation of this behavior would require further study of the precise energy band structure and its relationship with the transport properties of atomically thin CaF_2/Si heterostructures.

Using the material parameters of the thickness-dependent effective mass of CaF_2 and ΔE_C between Si and CaF_2 shown in Fig. 2 and the parameters shown in Table I, I-V curves with the negative differential resistance (NDR) of double-barrier resonant tunneling diode structures at RT were calculated as a parameter of the effective mass of CdF_2 (m^*_{CdF2}) and the thicknesses of the CaF_2 barriers with different layer thicknesses of t_1 and t_2. The layer thickness sequence of the device is n- Si(5.0 nm)/CaF_2(t_1 nm)/ CdF_2(2.5 nm)/CaF_2(t_2 nm)/i-Si(0.93 nm)/Al as shown in the inset of Fig. 3, where n-Si denotes As-doped n-type Si and i-Si denotes intrinsic (non-doped) Si. The plots of white circles (m^*_{CdF2} = 0.40 m_0), squares (0.38 m_0), triangles (0.36 m_0), and diamonds (0.34 m_0) indicate the calculated results of the relationship between the peak voltage and the peak current density of NDR characteristics. The solid circle indicates an experimental result reported in Ref. 5, which was well reproduced with the calculated result derived with the parameters m^*_{CdF2} = 0.36 m_0, t_1=0.62 nm (2ML), and t_2=0.93 nm (3ML). The typical literature value of m^*_{CdF2} is 0.4

m_0; however, the reason for the difference is open for discussion at the moment, although one possible reason considered is the thickness dependence of m* and another is the energy dependence of m* due to the deviation from the dispersion of the band structure of CdF_2 at the quasi-energy level of the quantum well, which is 1eV higher than that at the conduction band bottom. Figure 3 also suggests that a peak current density as high as $10^2 kA/cm^2$ is possible for a switching voltage less than 0.5 V where $t_1=t_2=0.62$ nm, which is important for high-current-density and low- voltage operation, although the optimum design configuration will be determined by optimization for specific applications.

In Fig. 4, the solid line shows the experimental I-V curve of the double-barrier structure from Ref. 5 and the dotted line indicates the calculation result of the I-V curve for the device structure using the parameters $m^*_{CdF2}=0.36\ m_0$, $t_1=0.62$ nm, and $t_2=0.93$ nm, and the values from Fig. 2 and Table I. In the result, V_{peak} was well fitted and the experimental J_{peak} is 75% of the calculated J_{peak}, presumably because the CaF_2 layer thickness deviation by a +1 monolayer in the area of 25% of the device resulted in the current reduction of one order of magnitude, as implied by Fig. 3.

Note that the thickness dependences of the effective mass of CdF_2 and the conduction band discontinuity between CaF_2 and CdF_2 would be more important, especially in determining the peak voltage as the CdF_2 layer thickness decreases, although they are assumed to be constant in this study. Therefore, further analysis, especially for material parameters of CdF_2, is required to improve the accuracy of the design of the I-V characteristics of the double-barrier or more complex device structures in the next stage of this study.

4. Conclusions

The current-voltage characteristics of the single-barrier Al/CaF_2/Si and double-barrier CaF_2/CdF_2/CaF_2 resonant tunneling diode structures were theoretically analyzed on the basis of the effective mass approximation and fitted with the measured I-V characteristics for the precise evaluation of ΔE_C and m* of atomically thin CaF_2 layers. As a result of the fitting simulation of the single-barrier tunneling structures, it was suggested that ΔE_C and m* vary with the CaF_2 layer thickness (t_{CaF2}), for example, m* = 1.0 m_0 and ΔE_C = 1.5 eV when t_{CaF2} = 0.93 nm , m* = 0.7 m_0 and ΔE_C = 1.7 eV when t_{CaF2} = 1.6 nm, and m* = 0.5 m_0 and ΔE_C = 2.1 eV when t_{CaF2} = 2.2 nm,indicating that the conduction band discontinuity of the Si/CaF_2 heterointerface decreases and the effective mass m* of CaF_2 increases with decreasing CaF_2 layer thickness. Using these results, the fitting simulation of the I-V characteristics of the double-barrier resonant tunneling diode structures was carried out. The effective mass of CdF_2 was evaluated to be 0.36 m_0, which well reproduced the peak voltage and the peak current density. The results obtained in this study will help us to further understand and precisely engineer the electron transport in atomically thin multilayered heterostructure devices.

Acknowledgments

The authors would like to thank Professor Emeritus Y. Suematsu, Professor Emeritus K. Iga, and Professor Emeritus K. Furuya for the continuous encouragement. The authors would also like to thank Professors S. Arai, M. Asada, Y. Miyamoto, and K. Tsutsui, and Associate Professors N. Nishiyama, S. Suzuki, S. Ohmi, K. Kakushima, and S. Sugahara for fruitful discussions. Moreover the authors would like to thank S. Tamura, D. Shoji, and

Y. Nagumo for technical assistance with laboratory equipment. This research was supported by the Ministry of Education, Culture, Sports, Science and Technology through a Grant-in-Aid for Scientific Research from the Japan Society for the Promotion of Science, and by the Research Center of Quantum Nanoelectronics.

References

1) A. Izumi, N. Matsubara, Y. Kushida, K. Tsutsui, and N. S. Sokolov, Jpn. J. Appl. Phys. **36**, 1849 (1997).
2) M. Watanabe, T. Funayama, T. Teraji, and N. Sakamaki, Jpn. J. Appl. Phys. **39**, L716 (2000).
3) M. Watanabe and T. Wada, Ext. Abstr. Solid State Devices and Materials, 2008, p. 1090.
4) J. Denda, K. Uryu, K. Suda, and M. Watanabe, Appl. Phys. Express **7,** 044103 (2014).
5) J. Denda, K. Uryu, and M. Watanabe, Jpn. J. Appl. Phys. **52,** 04CJ07 (2013).
6) A. Izumi, Y. Hirai, N. S. Sokolov, and K. Tsutsui, Appl. Phys. Lett. **67,** 2792 (1995).
7) T. Kanazawa, M. Watanabe, and M. Asada, Appl. Phys. Lett. **90,** 092101 (2007).
8) T. Kanazawa, A. Morosawa, R. Fuji, T. Wada, M. Watanabe, and M. Asada, Jpn. J. Appl. Phys. **46,** 3388 (2007).
9) Ph. Avouris and R. Wolkow, Appl. Phys. Lett. **55,** 1074 (1989).
10) J. Viernow, D. Y. Petrovykh, A. Kirakosian, J.-L. Lin, F. K. Men, M. Henzler, and F. J. Himpsel, Phys. Rev. B **59**, 10356 (1999).
11) A. Klust, T. Ohta, A. A. Bostwick, E. Rotenberg, Q. Yu, F. S. Ohuchi, and M. A. Olmstead, Phys. Rev. B **72**, 205336 (2005).
12) T. Sakaguchi, M. Watanabe, and M. Asada, IEICE Trans. Electron, **74**, 58 (1991).
13) R. Tsu and L. Esaki, Appl. Phys. Lett. **22**, 562 (1973).
14) I. Hase, H. Kawai, K. Kaneko and N. Watanabe, J. Appl. Phys. **59**, 3792 (1986)
15) H. Ohnishi, T. Inata, S. Muto, N. Yokoyama and A. Shibatomi, Appl. Phys. Lett. **49**, (1986) 1248.
16) Y. Ando and T. Itoh, J. Appl. Phys. **61**, 1497 (1987).

17) A. Izumi, Y. Hirai, N. S. Sokolov, and K. Tsutsui, Appl. Phys. Lett. **67**, 2792 (1995).

18) R. T. Poole and D. R. Williams, Chem. Phys. Lett. **36**, 401 (1975).

19) B. A. Orlowsky and J. M. Langer, Phys. Status Solidi B **91**, K53 (1979).

20) M. Watanabe, W. Saitoh, Y. Aoki, and J. Nishiyama, Solid-State Elec. **42**, 1627 (1998).

21) A. Izumi, K. Tsutsui, N. S. Solokov, N. N. Faleev, S. V. Gastev, S. V. Novikov, and N. L. Yakovlev, J. Cryst. Growth **150**, 1115 (1995).

22) N. S. Sokolov, N. N. Faleev, S. V. Gastev, N. L. Yakovlev, A. Izumi, and K. Tsutsui, J. Vac. Sci. Technol. A **13**, 2703 (1995).

23) B. Zhang, K. Furuya, Y. Ikeda and N. Kikegawa, Jpn. J. Appl. Phys. **38**, 4887 (1999).

24) M. I. Vexler N. S. Sokolov, S. M. Suturin, A. G. Banshchikov, S. E. Tyaginov and T. Grasser, J. Appl. Phys. **105**, 083716 (2009).

25) M. Depas, R. L. Meirhaeghe, W. H. Laflere and F. Cardon, Solid State Elec. **37**, 433 (1994).

26) M. Depas, B. Vermeire, P. W. Mertens, R. L. Van Meirhaeghe and M. M. Heyns, Solid State Elec. **38**, 1465 (1995)

27) M. Hirose, M. Hiroshima, T. Yasaka, M. Takakura and S. Miyazaki, Microelectron. Eng. **22**, 3 (1993).

28) S. –H. Lo, D. A. Buchanan, Y. Taur and W. Wang, IEEE Elec. Dev. Lett. **18**, 209 (1997).

29) Y. C. Yeo, Q. Lu, W. C. Lee, T.-J. King, C. Hu, X. Wang, X. Guo and T. P. Ma, IEEE Elec. Dev. Lett. **21**, 540 (2000).

Figure Captions

Fig. 1. Calculation results (solid and dashed lines) and experimental I-V plots of CaF_2 single-barrier tunneling diodes with barrier layer thicknesses of (i) 0.93, (ii) 1.6, and (iii) 2.2 nm. The inset shows the band diagram of the structure at an applied voltage of 1 V.

Fig. 2. Plots of ΔE_C and m* extracted by fitting simulation of I-V characteristics of single-barrier Al/CaF_2/Si tunneling diode structure. The value of the plots corresponding to the green diamond was cited from Ref. 23 evaluated using a scanning-tunneling-spectroscopy-based technique.

Fig 3. Peak voltage vs peak current density of negative differential resistance characteristics of double-barrier tunneling structure as parameters of effective mass for CdF_2 (m^*_{CdF2}) and the CaF_2 layer thicknesses (t_1 and t_2).

Fig. 4. I-V characteristics of double-barrier resonant tunneling diode structure: n-Si/CaF_2/CdF_2/CaF_2/i-Si/Al. The solid line shows the experimental result[5)] and the dotted line indicates the calculation result of the device structure using the parameters t_1=0.62 nm, t_2=0.93 nm, and m^*_{CdF2}=0.36 m_0.

Table I. Material parameters used in this study. ΔE_C, m^*_{CaF2} and m^*_{CdF2} are evaluated from the fitting simulation of the I-V characteristics.

Material	Relative permittivity	Effective mass	Conduction band discontinuity with Si [eV]
Si	11.8	0.26 m_0	0
CaF_2	6.76	m^*_{CaF2}	ΔE_C
CdF_2	8.83	m^*_{CdF2}	-0.6

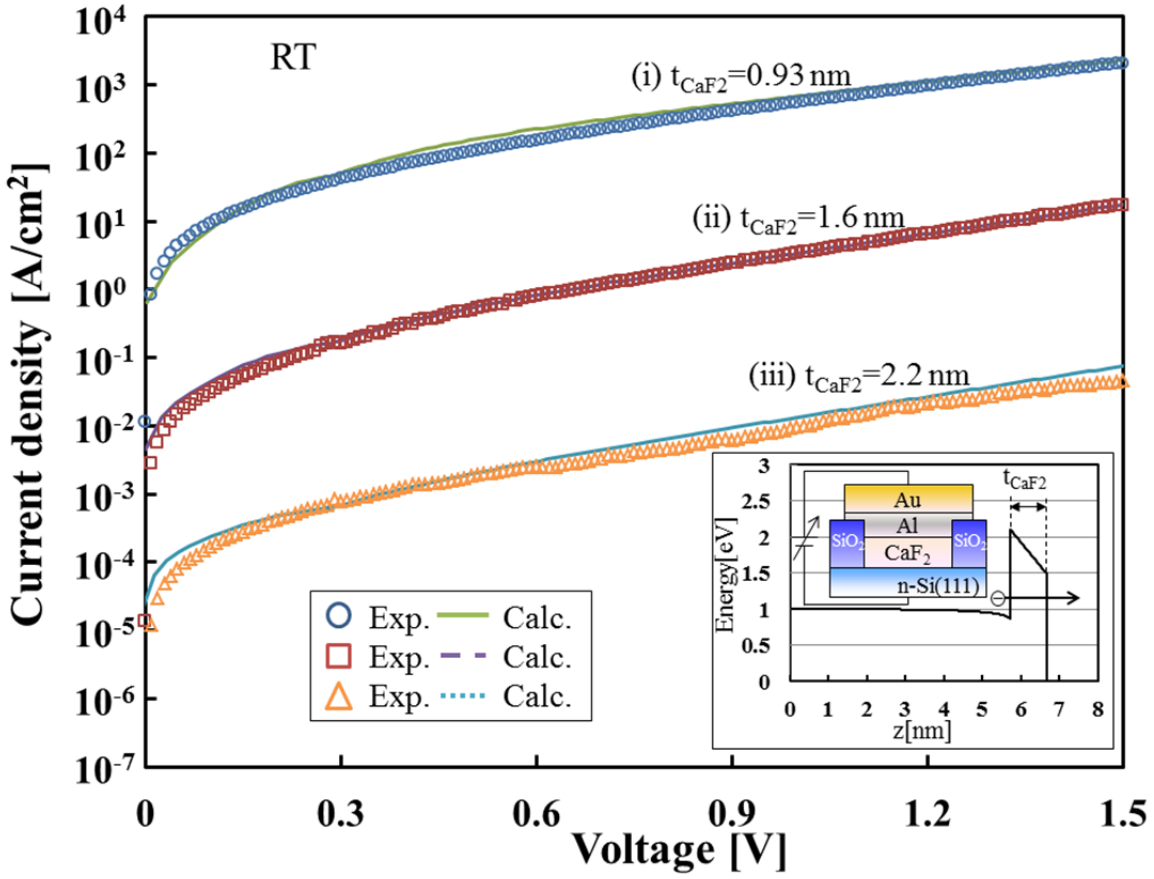

Fig. 1 K. Suda *et al.*

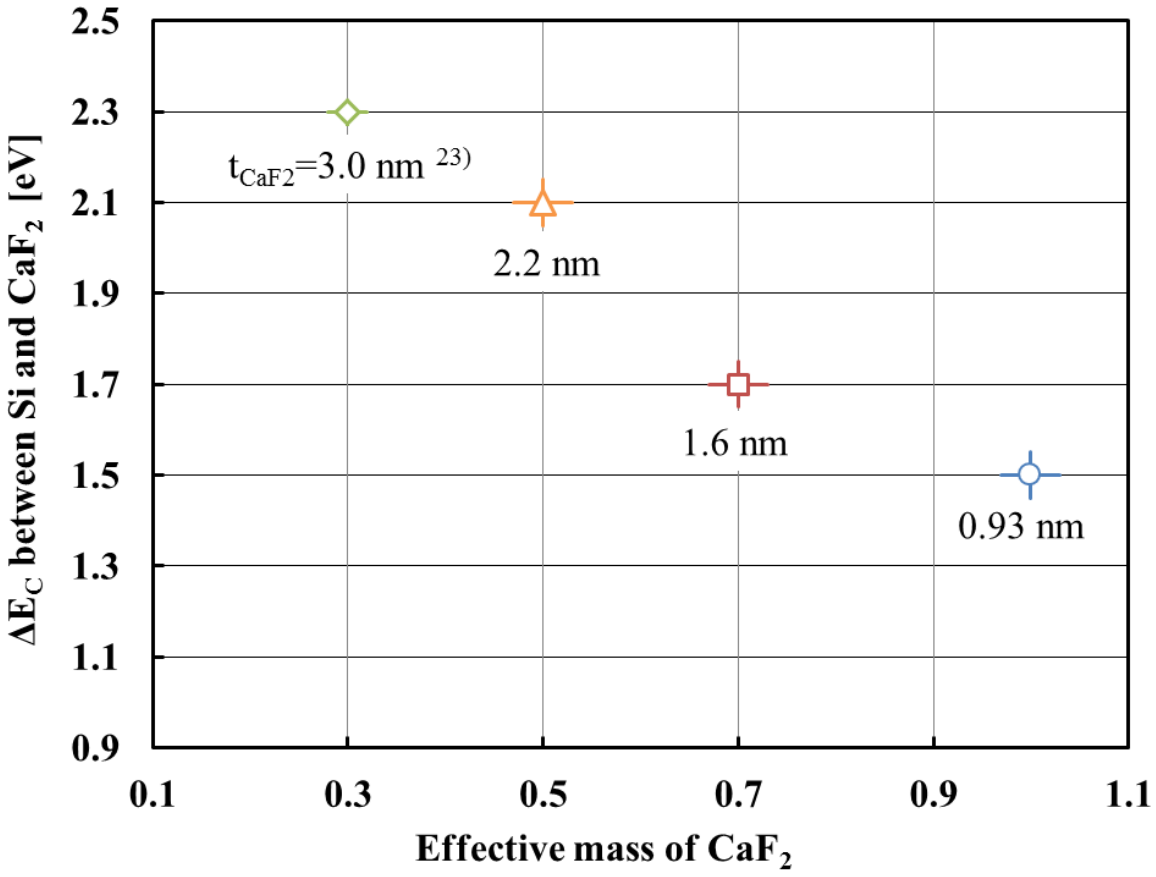

Fig. 2 K. Suda *et al.*

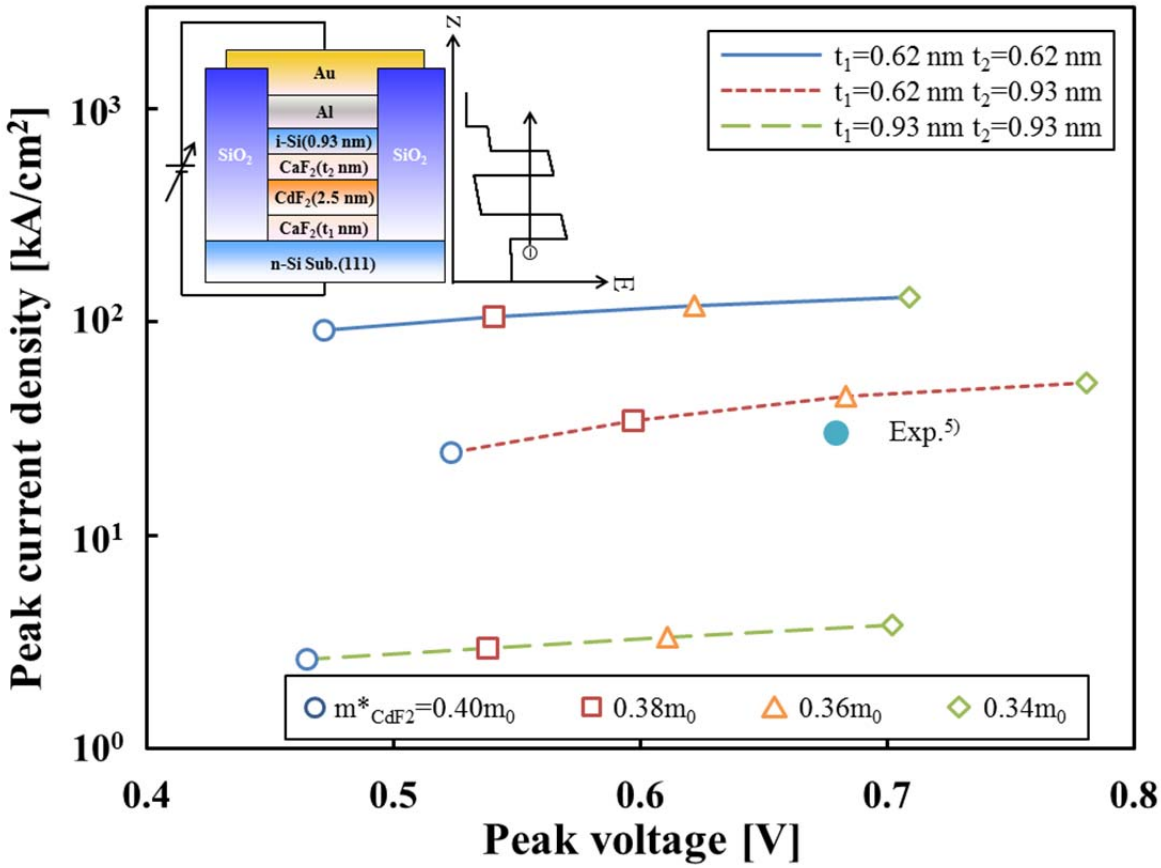

Fig. 3 K. Suda *et al.*

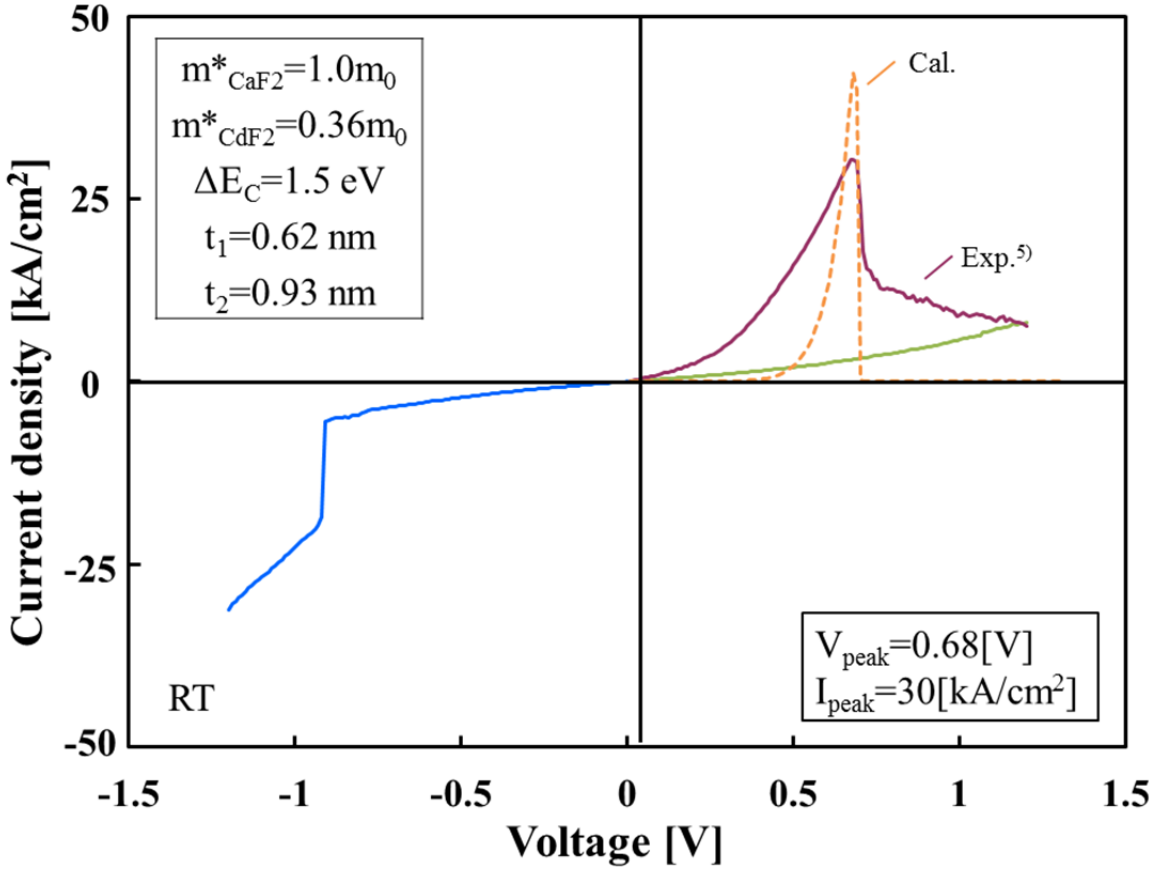

Fig. 4 K. Suda *et al.*